Journal of *Marine Science and Engineering*

MDPI

Article

Theoretical and Numerical Analysis of Ocean Buoy Stability Using Simplified Stability Parameters

Huiyuan Zheng [1,2], Yonghua Chen [1,*], Qingkui Liu [1], Zhigang Zhang [3,4], Yunzhou Li [4,5,*] and Min Li [4]

[1] Key Laboratory of Ocean Observation and Forecasting and Key Laboratory of Ocean Circulation and Waves, Institute of Oceanology, Chinese Academy of Sciences, Qingdao 266071, China
[2] National Ocean Technology Center, Tianjin 300112, China
[3] School of Mechanical Engineering, Shandong University, Jinan 250061, China
[4] Institute of Oceanographic Instrumentation, Qilu University of Technology (Shandong Academy of Sciences), Qingdao 266061, China; lm@sdioi.com
[5] Laoshan Laboratory, Qingdao 266237, China
* Correspondence: chenyonghua@qdio.ac.cn (Y.C.); lyz@qlu.edu.cn (Y.L.)

Abstract: The stability performance of the buoy is an important parameter that should be taken into account when designing marine buoys. This paper introduces a theoretical and numerical analysis method to examine the stability of marine buoys, including analysis of the initial stability and large inclination stability by calculating the natural period, metacentric height, static stability, and dynamic stability, deriving the calculation process of the static stability lever in detail to obtain the righting moment, and so on, showing that the designed buoy in this paper has sufficient stability performance with theoretically excellent resistance performance to the wind and waves. Additionally, the hydrodynamic performance of the buoy at different heights is also further analyzed for structural optimization, which concluded that the buoy would have a more balanced stability performance when the buoy's width-to-height ratio is 0.375–0.5, hoping that the computational model and ideas used in this paper can provide a reference for the theoretical stability analysis and buoy design of other types of buoys.

Keywords: marine buoy; stability performance; structural optimization; width-to-height ratio

Citation: Zheng, H.; Chen, Y.; Liu, Q.; Zhang, Z.; Li, Y.; Li, M. Theoretical and Numerical Analysis of Ocean Buoy Stability Using Simplified Stability Parameters. *J. Mar. Sci. Eng.* **2024**, *12*, 966. https://doi.org/10.3390/jmse12060966

Academic Editor: Md Jahir Rizvi

Received: 25 April 2024
Revised: 23 May 2024
Accepted: 30 May 2024
Published: 7 June 2024

1. Introduction

Long-term and real-time monitoring of the marine environment using marine monitoring buoys for marine environmental parameter data has obvious advantages, such as not being affected by the sea weather to a certain extent and carrying out sustainable marine monitoring activities. It could not only collect a variety of hydrometeorological elements but also obtain marine ecological environment, seawater materialization, and other parameters by carrying a variety of physical and chemical sensors to realize comprehensive monitoring of the overall water layer [1]. Obviously, long-term, multi-parameter profile and multi-layer observation and collection of marine environmental data can be achieved by anchoring the buoy in the characteristic sea area, which can provide necessary data support for marine environmental monitoring and protection, marine fishery resource development, marine engineering, and oceanographic research [2]. However, due to the changeable weather and complex sea conditions, the buoy is prone to swaying under the combined action of wind, waves, and currents, which have been shown to interact with one another to produce complex environmental conditions that would result in errors in the data collection of the sensors [3]. In a severe environment, the violent movement of the buoy will aggravate the fatigue of the buoy material and may even cause the buoy to overturn, which greatly affects the performance and life of the buoy system [4]. In addition, the deployment and maintenance of buoys need to consider large costs, so one of the most important problems when designing marine monitoring buoys is calculating the stability

of the buoy. The structure should be designed with good performance to cope with the sea environment, which can be used for better observation and data collection [5].

The stability of the marine buoy mainly refers to the ability of the buoy to deviate from the equilibrium position of the upright floating under the action of an external force and return to the equilibrium position of the initial positive floating after the external force disappears [6]. Generally, it can be studied by methods such as theoretical analysis, numerical simulation, and sea test experiments. When designing buoys, many scholars would not only apply theoretical calculations to obtain the stability parameters but also use numerical simulation to study the hydrodynamic stability performance of buoys under actual sea conditions, which is simulated on commercial software such as AWQA 14.0, Fluent, and CFD [7]. The former belongs to the category of statics, while the latter belongs to dynamics, and the combination of these two methods could more comprehensively analyze the movement of marine buoys at sea [8]. Since the buoy selected in this paper is still in the design stage, the theoretical stability performance of the selected buoy is studied by the analytical method of theoretical numerical calculation. In this way, not only the performance parameters of the designed buoy body can be found out, but also further optimization and improvement of the design scheme of the buoy can be proposed according to the calculation results.

2. Designed Parameters of the Buoy

2.1. The Basic Situation of the Buoy

The marine buoy designed in this paper is a cylindrical buoy, and the structure mainly includes the upper tower, the main floating body, the cabin, and the lower bracket, as shown in Figure 1. The design diagram is as follows: The main floating body is similar to a hollow cylinder with two ends open, with an outer diameter of 1.6 m, an inner diameter of 0.4 m, and a height of 0.6 m. It is mainly made of PE material, and the exterior is coated with a new type of anticorrosion material, epoxy resin coating, to avoid seawater corrosion. The hollow area with an inner diameter of 0.4 m in the middle of the main floating body can be used as a cabin to store instruments and batteries, and the height is slightly higher than that of the main floating body. The total weight of the equipment carried by the main floating body and the cabin is 400 kg.

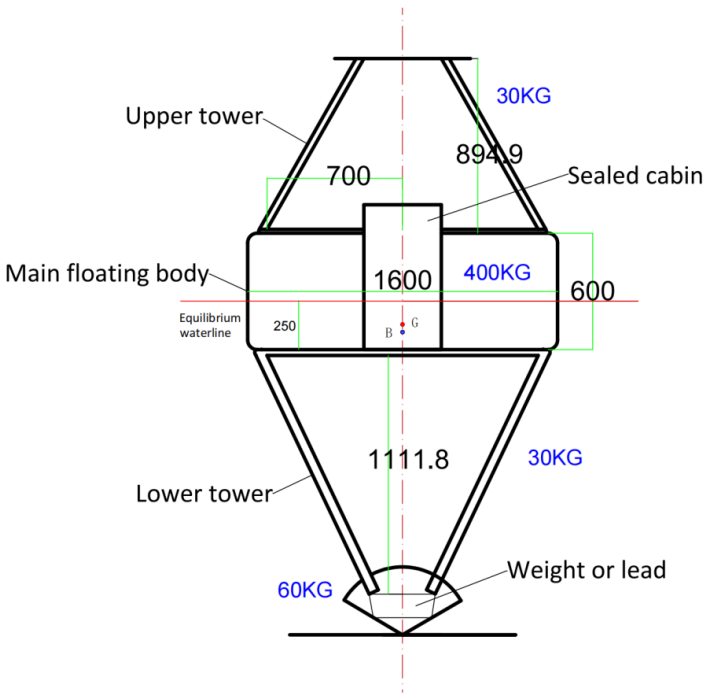

Figure 1. The overall design of the buoy.

The upper tower is mainly equipped with various hydrometeorological sensors, with a total weight of 30 kg. It is mainly made of aluminum alloy that has good support strength and good corrosion resistance, is low density, and is lightweight, which will not increase the overall center of gravity and enhance the stability of the buoy. The underwater part of the tower is made of stainless steel with a higher density and weighs 30 kg. There are two weights at the bottom welded to the fixed plate of the lower bracket and also equipped with sacrificial anode material, an anchorage connection ring, and other devices; the overall weight is up to 60 kg. In this way, the upper bracket is light and the lower bracket is heavy, which can further reduce the center of gravity and enhance the stability of the buoy.

2.2. Calculation of Various Buoy Parameters

2.2.1. Buoy Gravity Center, Waterline, and Buoyancy Center

Before starting to analyze the stability of the buoy, it is necessary to calculate some inherent properties of the buoy, including the center of gravity, the center of buoyancy, the position of the waterline and the displacement volume at equilibrium, the inherent rolling period, and the moment of inertia. The cylindrical buoy designed in this paper has good symmetry; it can be determined that the center of gravity is located on the central axis of the buoy, while the position of the center of gravity does not change with the change in the set coordinate system. Therefore, it is assumed that the bottom of the main floating body of the buoy is the datum plane, and after calculating the waterline surface at the initial balance, the waterline surface is used as the XOY plane, the central axis of the buoy at the time of balance is set as the Z axis, and the intersection of the line and the plane is the origin O, establishing the coordinate system for calculation.

Assuming that the total mass of the entire ocean buoy is M, for the convenience of calculation, the cabin and the main floating body are regarded as a whole with the same height, so their mass is M1. The center of gravity of the upper tower M2 and the lower tower M3 could be regarded as distributed in the center of the component, and if the weight at the bottom is M4, then the total mass M of the buoy and the position of the center of gravity of the whole Z_g are calculated as follows:

$$M = M1 + M2 + M3 + M4 = \sum_{i=1}^{4} M_i \tag{1}$$

$$Z_g = \frac{\sum_{i=1}^{4} M_i \times Z_i}{\sum_{i=1}^{4} M_i} = \frac{30 \times 105 - 30 \times 56 - 60 \times 112 + 400 \times 30}{520} \cong 13 \text{ cm} \tag{2}$$

Z_i is the distance from each component to the base plane of the bottom of the main floating body, the unit is cm; after bringing in the numerical value, it is obtained that the center of gravity Z_g is approximately 13 cm from the bottom of the main floating body.

When the object floating on the water is in equilibrium, the center of gravity and the center of buoyancy are on the same vertical line, which is the central axis of the buoy, and the drainage volume is approximately symmetrically distributed along the central axis. According to Archimedes' principle, the drainage volume V is calculated as follows:

$$\sum_{i=1}^{4} M_i \times g = \rho \times g \times V = \rho \times g \sum_{i=1}^{3} V_i \tag{3}$$

Among them, ρ is the density of seawater; take 1020 kg/m^3 offshore and bring it into the formula to obtain the total drainage volume V = 0.5098 m^3. Assuming that the drainage volume of the 20 cm × 20 cm × 25 cm weight is V_4 = 0.01 m^3 and the volume of stainless steel pipe with a 4 cm diameter is V_3 = 0.006 m^3, the drainage volume of the main floating body is V_1 = 0.4938 m^3. Bring the value into the cylinder volume formula $V_1 = \pi \times r^2 \times h$, could obtain h = 24.6 cm. In order to facilitate the calculation, take h = 25 cm, that is, the buoy water surface line is 25 cm from the bottom datum surface.

The center of buoyancy, b, is defined as the center of gravity of the fluid displaced by the object immersed in the fluid, whose position is expressed in the Cartesian coordinate system as follows:

$$Z_b = \frac{\iiint z_i \times dV}{\iiint dv} = \frac{\sum_{i=1}^{3} V_i \times h_i}{\sum_{i=1}^{3} V_I} \quad (4)$$

where h_i is the distance from the volume of fluid displaced by the part immersed in water to the waterline, then, $Z_b \cong 15.94$ cm $\cong 16$ cm is calculated, that is, the center of buoyancy on the Z axis is 16 cm below the positive floating water line and 9 cm above the base surface of the main floating body.

2.2.2. Initial Stability

The stability of marine buoys usually includes the initial stability of the buoy and its stability at large angles of inclination. The former refers to stability when the inclination angle is less than 10°, and the latter refers to stability when the inclination angle is greater than 10° [9]. As shown in Figure 2, after the buoy is tilted by an angle of φ under the action of an external force, its center of buoyancy B will move to a new position along a certain curve, which is Bφ. The angle between the waterline W_0L_0 at equilibrium and the waterline $W_\varphi L_\varphi$ at tilt is φ. The vertical line of the new center of buoyancy B_φ will intersect the central axis of the buoy at point m, which is called the metacenter of the buoy. The moment of the buoy is present as follows:

$$M = M \times \overline{gm} \times \sin\varphi \quad (5)$$

where $\overline{gm}$ is the distance between the center of gravity G and the metacenter m, which is also called the metacentric height; M is the displacement.

When the metacenter m is above the center of gravity G, the righting moment will straighten the floating back to the equilibrium position, and otherwise, the buoy will have the possibility of overturning.

Obviously, it is difficult to calculate $\overline{gm}$, but it can be obtained indirectly by calculating the distance between the center of buoyancy B and the metacenter m. The calculation formulas are given below:

$$\overline{bm} = \frac{I}{V} \quad (6)$$

$$I = \int y^2 dy = \frac{\pi \times D^4}{64} \quad (7)$$

$$\overline{gm} = \overline{bm} \pm \overline{gb} \quad (8)$$

where I is indicated as the moment of inertia of the waterline facing the transverse axis of the waterline surface, V is the volume of the water discharged by the buoy, and D is the diameter of the main floating body. When the inclination angle is small, the change curve of the center of buoyancy B is similar to an arc, so it is also called the metacentric radius of the buoy. And then $I = 0.3217$ m^4 is calculated as follows:

$$\overline{bm} = \frac{0.3217}{0.5098} = 0.631 \text{ m};$$

$$\overline{gm} = 0.6310 - \frac{13-9}{100} = 0.591 \text{ m};$$

The metacentric height is one of the important indicators to measure the initial stability of the buoy [10,11]. For the industry standard for the initial stability of marine floating structures, the initial stability height should not be less than 0.15 m. From the above results, the initial metacentric height of the marine buoy designed in this paper meets this requirement.

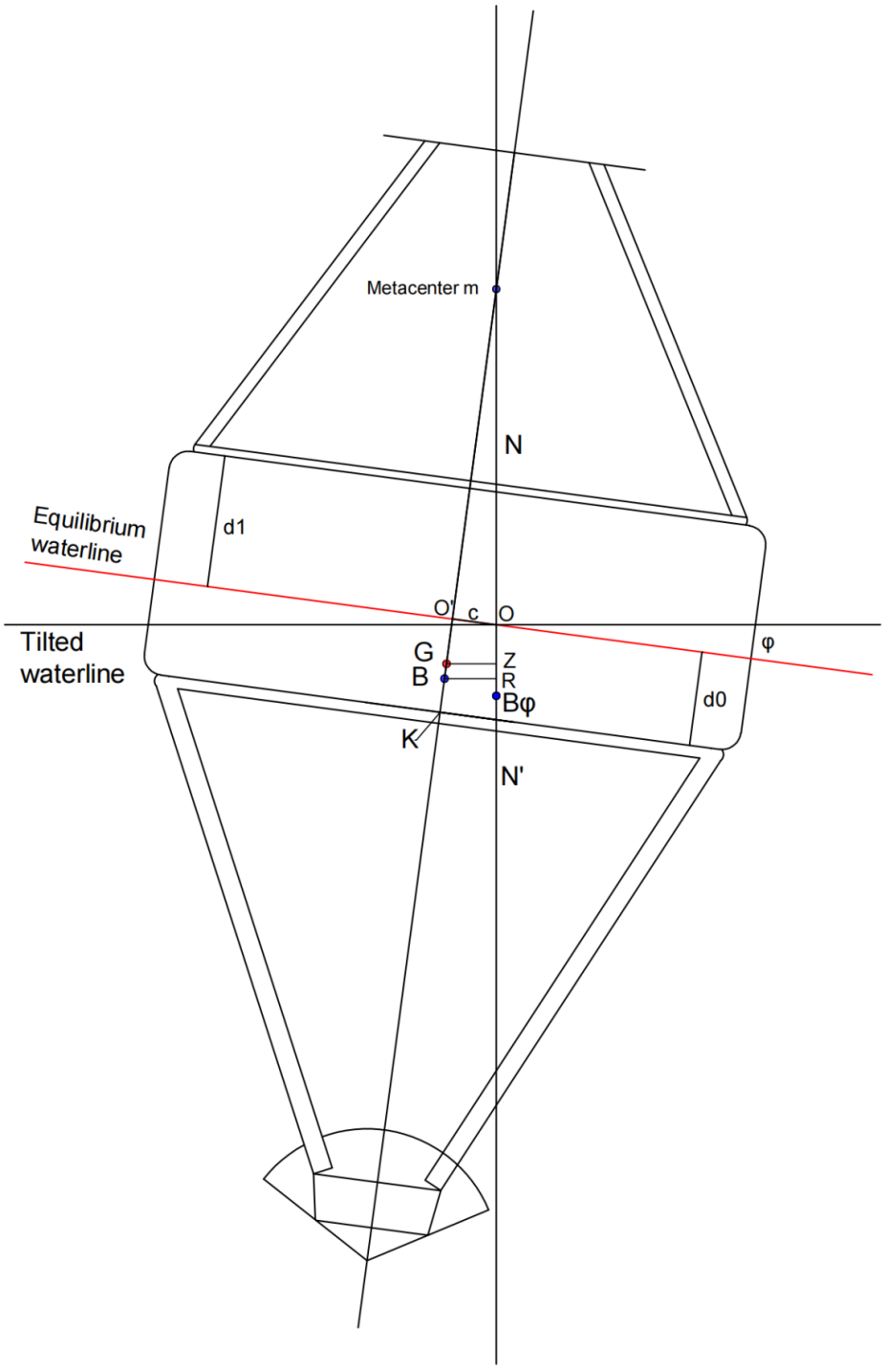

Figure 2. The derivation process of the metacenter height.

2.2.3. Natural Rolling Period of Buoy

The tilted buoy with a righting moment will perform an undamped rolling motion under ideal conditions and then gradually return to equilibrium due to the internal damping having little impact on their rolling stability in the nonresonance region [12]. Considering the volume element dv with mass m on the main floating body, its distance from the horizontal axis passing through the center of gravity is r, by moving at a speed of v so that

$\vec{v} = \vec{\omega} \times \vec{r}$ and angular velocity $\vec{\omega} = \frac{d\varphi}{dt} = \dot{\theta}$. Then, the inertial force and inertial moment elements on the volume element are [13,14] as follows:

$$d\vec{F} = \frac{d}{dt}\left(m\vec{v}\right) = m\dot{\omega} \times \vec{r} \tag{9}$$

$$dM = m\vec{r} \times \dot{\omega} \times \vec{r} \tag{10}$$

The total moment of inertia is the integral over the entire buoy body, then

$$M = \iiint m\vec{r} \times \dot{\omega} \times \vec{r}\, dv = I_v \dot{\omega} = I_v \ddot{\varphi} \tag{11}$$

where I is the moment of inertia of the entire buoy about its axis through the center of gravity. Considering the rotational moment of inertia added by the water attached to the buoy during the rotation, a corresponding virtual moment of inertia I_v is introduced $I_v = I + I'$, where $I' = (0.2 \sim 0.4) \times I$ is the moment of inertia due to the attached water mass, whose specific value is related to its shape. Thus, the resulting moment of inertia is equal to the righting moment of the buoy in the opposite direction, that is $I_v\ddot{\varphi} + M \times \overline{gm} \times \sin\varphi = 0$. In the case of a small angle, $\sin\varphi \approx \varphi$, the equation can be simplified to $I_v\ddot{\varphi} + M \times \overline{gm} \times \varphi = 0$, which will obtain the differential equation of undamped free simple harmonic oscillation, as follows:

$$\ddot{\varphi} + \frac{M \times \overline{gm} \times \varphi}{I_v} = 0 \tag{12}$$

Then, the natural rolling frequency of the buoy is $f_0 = \frac{1}{2\pi}\sqrt{\frac{M \times \overline{gm}}{I_v}}$, and the natural rolling period is $T_0 = 2\pi\sqrt{\frac{I_v}{M \times \overline{gm}}}$.

The key to calculating the natural frequency is the virtual moment of inertia, usually considering the attachment mass-induced moment of inertia I', whose value is $0.2 \times I$, and I is the moment of inertia of the axis over the center of gravity parallel to the X/Y axis.

The moment of inertia of the main floating body can be obtained from the calculation formula of the moments of inertia of the cylinder around the X/Y axis and the parallel axis theorem, which is $I_1 = \frac{1}{4}mR^2 + \frac{1}{12}mh^2 + mD^2$, where h is the height of the main floating body, and D is the distance from the horizontal central axis of the floating body to the center of gravity G. The other components' moments of inertia are given as $I_i = M_i \times d^2$, where d is the distance from each component to the center of gravity G. Hence, the natural rolling period of the buoy is calculated as T_0 = 2.2 s. However, regardless of the actual conditions, the motion of buoys in seawater will be dampened to a certain extent, so the hydrodynamic nonlinear damping motion of buoys should be further studied in future studies.

2.2.4. Movement of the Buoy in the Wave

Assuming a sine wave propagating forward from the origin to the X-axis, whose expression can be written as follows [13]:

$$y = \frac{H}{2}\cos 2\pi\left(\frac{t}{T} - \frac{x}{L}\right) \tag{13}$$

Hence, the slope of this wave is as follows:

$$\frac{dy}{dx} = \tan\beta = \frac{\pi H}{L}\sin 2\pi\left(\frac{t}{T} - \frac{x}{L}\right) \tag{14}$$

When x = 0, the slope at this moment is as follows:

$$\beta \cong \tan\beta = \frac{\pi H}{L}\sin 2\pi\left(\frac{t}{T}\right) = \frac{\pi H}{L}\sin \omega t \tag{15}$$

The righting moment of the buoy in the waves changes as $M = M \times \overline{gm} \times \sin(\varphi - \beta)$, φ is the roll angle of the buoy, and β is the slope of the wave. In the case where both of them are small, it can be simplified to $M = M \times \overline{gm} \times (\varphi - \beta)$. Therefore, the equation of motion can be represented as follows:

$$I_v \ddot{\varphi} + M \times \overline{gm} \times (\varphi - \beta) = 0 \tag{16}$$

$$\ddot{\varphi} + \frac{M \times \overline{gm} \times \varphi}{I_v} = \frac{M \times \overline{gm}}{I_v} \times \frac{\pi H}{L} \sin \omega t \tag{17}$$

where the initial conditions are $\varphi_0 = \dot{\varphi}_0 = 0$, then the solution of the differential equation can be obtained as follows:

$$\varphi = \frac{\frac{\pi H}{L}}{1 - \frac{{T_0}^2}{T^2}} \left(\sin \omega t - \frac{T_0}{T} \sin \omega_0 t \right) \tag{18}$$

The maximum free-rolling angle is as follows:

$$\varphi_{max} = \frac{\frac{\pi H}{L}}{1 - \frac{{T_0}^2}{T^2}} = \frac{\pi H}{L} \left(\frac{T^2}{T^2 - {T_0}^2} \right) \tag{19}$$

It can be seen from the analytical formula that when the natural rolling period T_0 of the buoy and the period T of the wave are close to the same, they will suddenly increase and tend to be infinite, which will lead to the buoy resonating with the wave [15]. Therefore, when designing, the natural period of the buoy should avoid the period value of the wave as much as possible. The buoy designed in this paper will be placed in a certain area of the Bohai Sea in China. According to statistics, the maximum wave height in this area is 8 m, the wave period is 8.5 s, and the wavelength is 84 m. Hence, the maximum free rolling angle is 19.14°, which is the result calculated without damping. In the actual ocean, the buoy is subjected to seawater and other damping effects, so the real maximum free rolling angle will be smaller than this result.

2.3. Stability at a Large Angle of Inclination

The stability of the buoy at a large inclination angle refers to whether the restoring moment of the buoy can prevent itself from overturning after the buoy is tilted at a large angle under the action of an external force. Therefore, as with the initial stability, it is necessary to calculate the righting moment at large inclination angles, specifically the static stability lever curve and the dynamic stability lever curve. As shown in Figure 3 below, assuming that the buoy is in static water and affected by static force, the water line is horizontal. For cylindrical buoys, the coupling action of vertical tilt can be basically ignored, and only the rolling action is considered. The righting moment of the float can be defined as follows:

$$M_R = M \times \overline{GZ} \tag{20}$$

In initial stability, the static stability lever $\overline{GZ} = \overline{gm} \times \sin\varphi$, but as the inclination angle increases, the metacenter changes with the change in the volume of water entering and leaving, and the static stability lever is no longer $= \overline{gm} \times \sin\varphi$. Therefore, it is necessary to recalculate the righting lever $\overline{GZ}$. Quoting the theory of ship statics, the concept of the assumed center of gravity S is introduced, which stipulates that the assumed center of gravity S will not change due to the loading situation of the instruments carried by the upper and lower towers of the buoy.

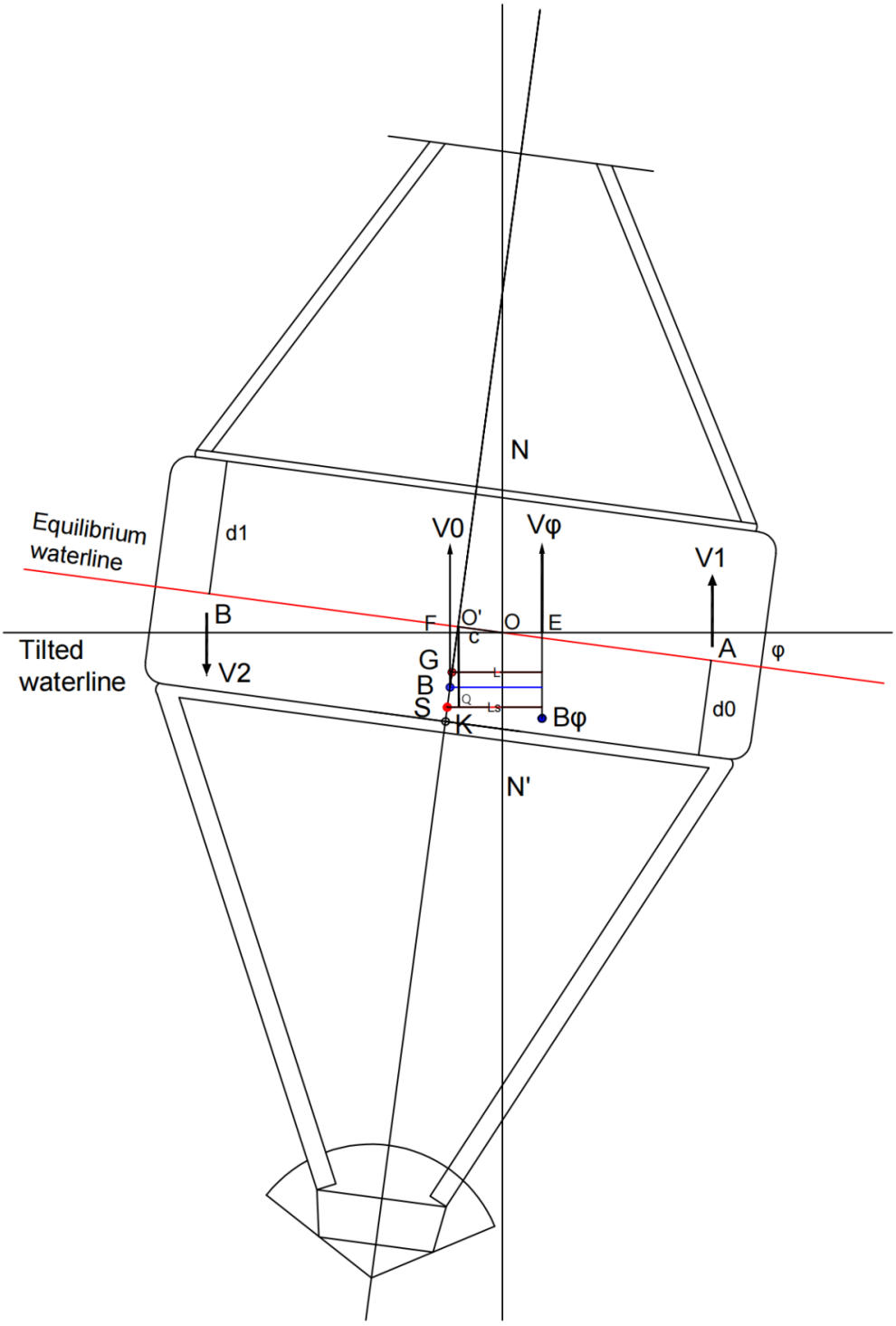

Figure 3. Schematic diagram of the derivation process of the static stability lever.

The calculation of the distance L_s from the buoyancy line of action to the S point after the buoy is given by the following equation:

$$L_s = \overline{OE} + \overline{OO'} + \overline{SQ} = l_\varphi + c\cos\varphi + (d_0 - \overline{KS})\sin\varphi \quad (21)$$

The l_φ is the distance from the buoyancy line of action to the reference axis NN′, and point Q is the intersection of the vertical line from point O′ with the horizontal vertical line

from point S. The static stability lever L can then be calculated according to the center of gravity G correction of the actual buoy loading situation, which is as follows:

$$\begin{aligned} \mathrm{L} &= \mathrm{L}_s - \overline{SG}\sin\varphi = \mathrm{L}_s - \left(\overline{KG} - \overline{KS}\right)\sin\varphi \\ &= l_\varphi + \mathrm{c}\cos\varphi + \left(\mathrm{d}_0 - \overline{KS}\right)\sin\varphi - \left(\overline{KG} - \overline{KS}\right)\sin\varphi \end{aligned} \tag{22}$$

2.3.1. Distance l_φ from the Center of Buoyancy to the Reference Axis

First of all, to facilitate the calculation, ignore the volume of the upper and lower brackets entering or leaving water and only consider the change in immersed wedge volume and emerged wedge volume of the main floating body. In Figure 3, after the buoy is heeled by the external force, the displacement volume of the buoy at this time changes as

$$\mathrm{V}_\varphi = \mathrm{V}_0 + \mathrm{V}_1 - \mathrm{V}_2 \tag{23}$$

where V_0 is the volume of drainage of the buoy at equilibrium, V_1 is the immersed wedge volume of the main floating body, and V_2 is the emerged wedge volume of the main floating body.

Then, the static moment of the inclined drainage volume concerning the reference axis NN′ can be obtained as follows:

$$\mathrm{M}_\varphi = \mathrm{V}_\varphi \times \overline{OE} = \mathrm{V}_1 \times \overline{OA} + \mathrm{V}_2 \times \overline{OB} - \mathrm{V}_0 \times \overline{OF} \tag{24}$$

Hence,

$$l_\varphi = \overline{OE} = \frac{\mathrm{M}_\varphi}{\mathrm{V}_\varphi} = \frac{\mathrm{V}_1 \times \overline{OA} + \mathrm{V}_2 \times \overline{OB} - \mathrm{V}_0 \times \overline{OF}}{\mathrm{V}_0 + \mathrm{V}_1 - \mathrm{V}_2} \tag{25}$$

where $\overline{OA}$ is the distance from the centroid of the immersed wedge volume to the reference axis NN′, $\overline{OB}$ is the distance from the centroid of the emerged wedge volume to the reference axis NN′, and $\overline{OF}$ is the distance from the drainage volume of the buoy at stable equilibrium to the reference axis NN′.

Obviously, $\overline{OF}$ could be expressed as follows:

$$\overline{OF} = \overline{FO'} + \overline{O'O} = \left(\mathrm{d}_0 - \overline{KB_0}\right)\sin\varphi + \mathrm{c}\cos\varphi \tag{26}$$

where d_0 is the distance h = 25 cm from the waterline plane to the base plane at the bottom of the main floating body in stable equilibrium, $\overline{KB_0}$ is the vertical distance from the datum plane of the main floating body to the center of buoyancy at equilibrium, $\overline{KB_0}$ = 9 cm, O′ is the intersection point of the waterline at equilibrium and the central axis of the buoy, point O is the intersection of the waterline at an inclination, and the reference axis NN′, also known as the center of floatation. The deviation value of the floatation center is an empirical value that is related to the position of the waterline, so the deviation value c is taken as 0.05 m in this paper. In this way, it is only necessary to calculate the immersed and emerged volume V_1, V_2, and the location of its centroids A and B to obtain l_φ and static stability lever L.

2.3.2. Volume and Centroid of Immersed Wedge and Emerged Wedge

The shape and centroid of the immersed wedge and emerged wedge are related to the inclination angle of the buoy. Considering the edge immersing and emerging seawater, the situation with the angle of edge immersion can be divided into three cases. Case 1, when the inclination angle is less than 17°, the shape of the immersed and emerged wedge, similar to the cylindrical cone, is the geometry of one part of the oblique truncated cylinder, which is relatively regular and illustrated in Figures 4 and 5. Case 2, when the inclination angle is greater than 17° and less than 25°, the immersed wedge volume does not change, while the emerged wedge volume is composed of a triangular prism-like geometry and an arcuate geometry with an arcuate base area and a height of d_0, which is part of a cylinder. Case 3, when the inclination angle is greater than 25°, the shape of both is the same and

composed of a triangular prism-like geometry and an arcuate geometry with an arcuate base area and a height of d_0 or d_1, just as Figures 4–6 shows.

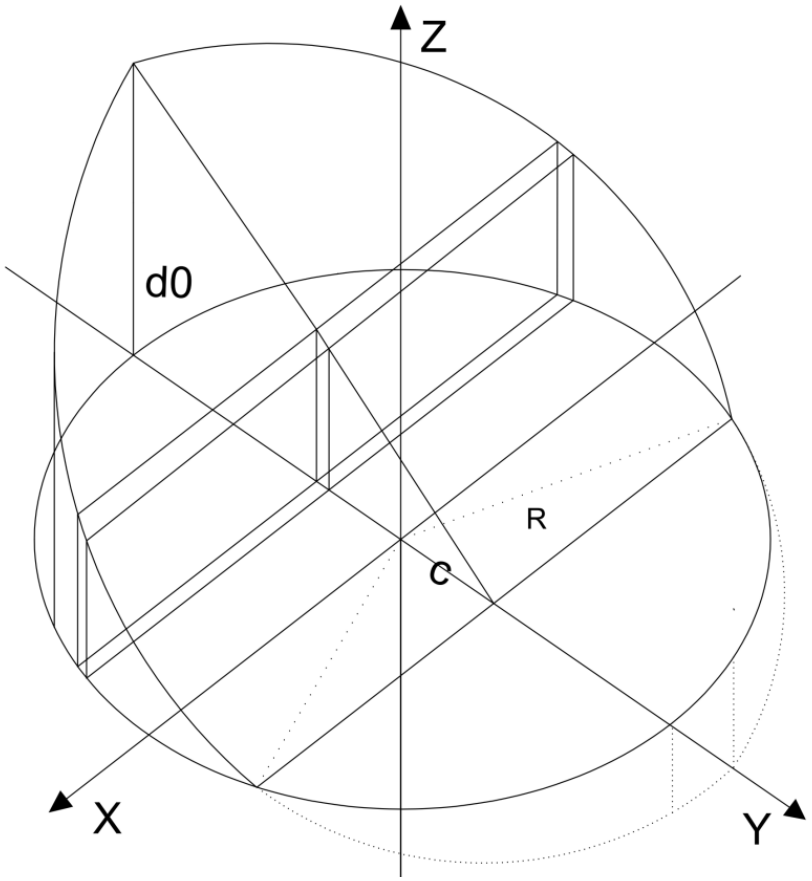

Figure 4. Immersed and emerged wedge volume (case 1).

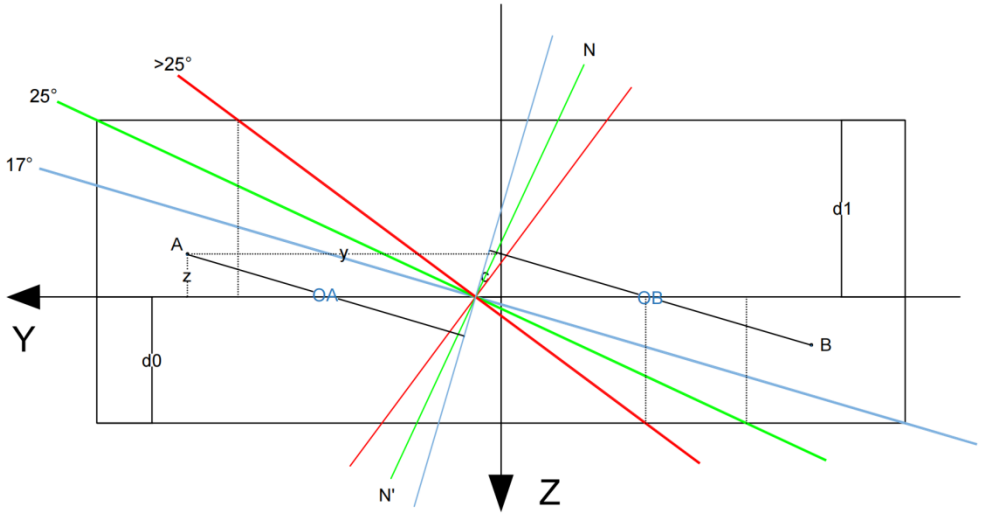

Figure 5. Three tilting situations of the buoy.

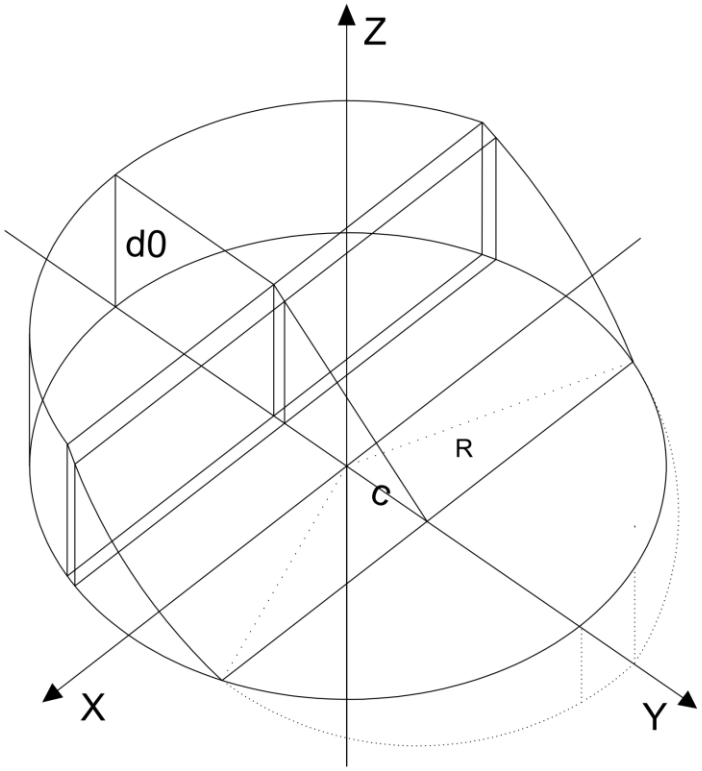

Figure 6. Immersed and emerged wedge volume (cases 2 and 3).

1. When $\varphi \leq 17^\circ$, the calculation formula for the volume of the main floating body entering or leaving the seawater wedge, similar to a cylindrical cone, can be derived as follows:
The infinitesimal volume of the emerged wedge:

$$dv_2 = x \times z \times dy, x = \sqrt{R^2 - y^2}, z = (c - y) \times \tan\varphi \tag{27}$$

Hence,

$$V_2 = \int_{-R}^{c} 2 \times (c - y) \times \tan\varphi \times \sqrt{R^2 - y^2} dy \tag{28}$$

The infinitesimal volume of the immersed wedge:

$$dv_1 = x \times z \times dy, x = \sqrt{R^2 - y^2}, z = (y - c) \times \tan\varphi \tag{29}$$

Therefrom

$$V_1 = \int_{c}^{R} 2 \times (y - c) \times \tan\varphi \times \sqrt{R^2 - y^2} dy \tag{30}$$

2. When $17^\circ \leq \varphi \leq 25^\circ$, V_2 volume consists of a triangular prism-like geometry V_{21} and one part of a cylinder V_{22}, where V_{21} is the same as the above formula with different integral domains and illustrated in Figure 6, which are written as follows:

$$V_{21} = \int_{c - \frac{d_0}{\tan\varphi}}^{c} 2 \times (c - y) \times \tan\varphi \times \sqrt{R^2 - y^2} dy \tag{31}$$

$$V_{22} = \frac{d_0 * R^2}{2} \times \left(2 \times \cos^{-1} \frac{\frac{d_0}{\tan\varphi} - c}{R} - \sin\left(2 \times \cos^{-1} \frac{\frac{d_0}{\tan\varphi} - c}{R} \right) \right) \tag{32}$$

where the arcuate area can be written as $S = \frac{R^2 \times (A - \sin A)}{2}$, A is the angle of the corresponding arc, and $A = 2 \times \cos^{-1} \frac{\frac{d_0}{\tan \varphi} - c}{R}$ in emerged wedge volume, then $V_2 = V_{21} + V_{22}$. At this moment, V_1 does not change, $V_1 = \int_c^R 2 \times (y - c) \times \tan \varphi \times \sqrt{R^2 - y^2} dy$.

3. When $25^\circ \leq \varphi$, the calculation of V_2 is as same as Case 2, and the integral domain is only modified by the change in the inclination angle. At this point, the shape of V_1 becomes the same as that of V_2, so that the formula for V_1 is written as follows:

$$V_{11} = \int_c^{\frac{d_1}{\tan \varphi} + c} 2 \times (y - c) \times \tan \varphi \times \sqrt{R^2 - y^2} dy \tag{33}$$

$$V_{12} = \frac{d_1 * R^2}{2} \times \left(2 \times \cos^{-1} \frac{\frac{d_1}{\tan \varphi} + c}{R} - \sin \left(2 \times \cos^{-1} \frac{\frac{d_1}{\tan \varphi} + c}{R} \right) \right) \tag{34}$$

Then, $V_1 = V_{11} + V_{12}$.

2.3.3. The Centroid of the Immersed or Emerged Wedge Volume

The centroid is only related to the shape of the object. Due to the symmetry of the cylindrical buoy, the position of the centroid must be on the Y0Z plane. It is only needed to calculate the coordinates on the Y and Z axes. The differential equation of a centroid is defined as follows:

$$\overline{y} = \frac{M_y}{V} = \frac{\iiint y \times dv}{\iiint dv} = \frac{\sum y_i \times V_i}{\sum V_i}; \overline{z} = \frac{M_z}{V} = \frac{\iiint z \times dv}{\iiint dv} = \frac{\sum z_i \times V_i}{\sum V_i} \tag{35}$$

In this formula, M_y and M_z are the static moments of the volume on the Y or Z axes, and the volume V has been obtained in the previous section.

1. The static moments to the Y or Z axes of one part of the emerged wedge volume are calculated as follows:

$$M_{21y} = \int 2 \times (c - y) \times \tan \varphi \times \sqrt{R^2 - y^2} \times y \, dy \tag{36}$$

$$M_{21z} = \int 2 \times (c - y) \times \tan \varphi \times \sqrt{R^2 - y^2} \times (c - y) \times \tan \varphi \, dy \tag{37}$$

The static moments to the Y or Z axes of one part of the immersed wedge volume are calculated as follows:

$$M_{11y} = \int 2 \times (y - c) \times \tan \varphi \times \sqrt{R^2 - y^2} \times y \, dy \tag{38}$$

$$M_{11z} = \int 2 \times (y - c) \times \tan \varphi \times \sqrt{R^2 - y^2} \times (y - c) \times \tan \varphi \, dy \tag{39}$$

Thus, one part of the centroid coordinates of the wedge-shaped volume can be obtained by dividing the calculated static moment by the volume.

2. The other part of the wedge-shaped volume is part of a complete cylinder, with good symmetry, and its z-coordinate of the centroid is $\overline{z} = \frac{h}{2}$, where h is the height of the cylinder. The centroid coordinate $\overline{y}$ of this geometry is the centroid coordinate y of the arcuate base, which can be solved by using polar coordinates. The arcuate area and area moment of the immersed wedge volume can be written as follows:

$$S_{12} = \int_{-\cos^{-1} \frac{\frac{d_1}{\tan \varphi} + c}{R}}^{\cos^{-1} \frac{\frac{d_1}{\tan \varphi} + c}{R}} \int_{R \cos \varphi}^{R} r \, dr d\theta \tag{40}$$

$$M_{12} = \int_{-\cos^{-1}\frac{\frac{d_1}{\tan\varphi}+c}{R}}^{\cos^{-1}\frac{\frac{d_1}{\tan\varphi}+c}{R}} \int_{R\cos\varphi}^{R} r \times \cos\theta \times r \, dr d\theta \tag{41}$$

Hence,

$$\overline{y_{12}} = \frac{M_{12}}{S_{12}} \tag{42}$$

The arcuate area and area moment of the emerged wedge volume can be written as follows:

$$S_{22} = 2 \times \int_{0}^{\cos^{-1}\frac{c-\frac{d_0}{\tan\varphi}}{R}} \int_{R\cos\varphi}^{R} r \, dr d\theta \tag{43}$$

$$M_{22} = 2 \times \int_{0}^{\cos^{-1}\frac{c-\frac{d_0}{\tan\varphi}}{R}} \int_{R\cos\varphi}^{R} r \times \cos\theta \times r \, dr d\theta \tag{44}$$

Hence,

$$\overline{y_{22}} = \frac{M_{22}}{S_{22}} \tag{45}$$

After obtaining the centroid coordinates of the two geometric bodies, the above (35) formula may be used to determine the ultimate centroid position of the entire immersed or emerging wedge volume as Equation (35).

When the buoy is tilted by φ angle, the equation for the reference axis NN′ is defined as $-\frac{1}{\tan\varphi}y + z - \frac{c}{\tan\varphi} = 0$, which can be solved for $\overline{OA}$ and $\overline{OB}$ using the distance formula from point to line.

$$d_i = \frac{\left|-\frac{1}{\tan\varphi} \times \overline{y} + \overline{z} - \frac{c}{\tan\varphi}\right|}{\sqrt{\left(-\frac{1}{\tan\varphi}\right)^2 + 1}} \tag{46}$$

Finally, by bringing $V_1, V_2, \overline{OA}, \overline{OB}$ into the equation $l_\varphi = \frac{V_1 \times \overline{OA} + V_2 \times \overline{OB} - V_0 \times \overline{OF}}{V_0 + V_1 - V_2}$ to calculate l_φ, and then taking l_φ into the above (22) equation, we could obtain the static stability lever.

$$\begin{aligned} L &= L_s - \overline{SG}\sin\varphi = L_s - \left(\overline{KG} - \overline{KS}\right)\sin\varphi \\ &= l_\varphi + c\cos\varphi + \left(d_0 - \overline{KS}\right)\sin\varphi - \left(\overline{KG} - \overline{KS}\right)\sin\varphi \end{aligned} \tag{47}$$

3. Discussion of Static Stability Curve and Dynamic Stability Curve

3.1. Static Stability Curve

The static stability arm with an inclination angle interval of 5° and a range of 5° to 85° may be obtained and presented as a graph in Figure 7 using the calculation method from the previous section. It is generally considered that small marine buoys should meet the following requirements: 1. The initial metacentric height shall not be less than 0.15 m, 2. The stability arm when heeling 30° shall be greater than 0.2 m, and 3. The stability vanishing angle shall be greater than 55°. Obviously, it can be seen from Figure 7 that all the buoys designed in this paper meet these conditions.

When the slope on the static stability curve is 0, the corresponding highest point is the maximum static inclination moment (lever l_{max}) that the buoy can withstand, that is, the maximum restoring moment (arm) possessed by the buoy, and the corresponding heel angle is the limit static inclination angle φ_{max}. The trend of the restoring moment or righting moment $M_R = M \times L$ of the buoy is the same as that of the static stability lever curve. When the angle of inclination $\varphi < \varphi_{max}$, the buoy is still in a stable equilibrium state; otherwise, it is in an unstable equilibrium state.

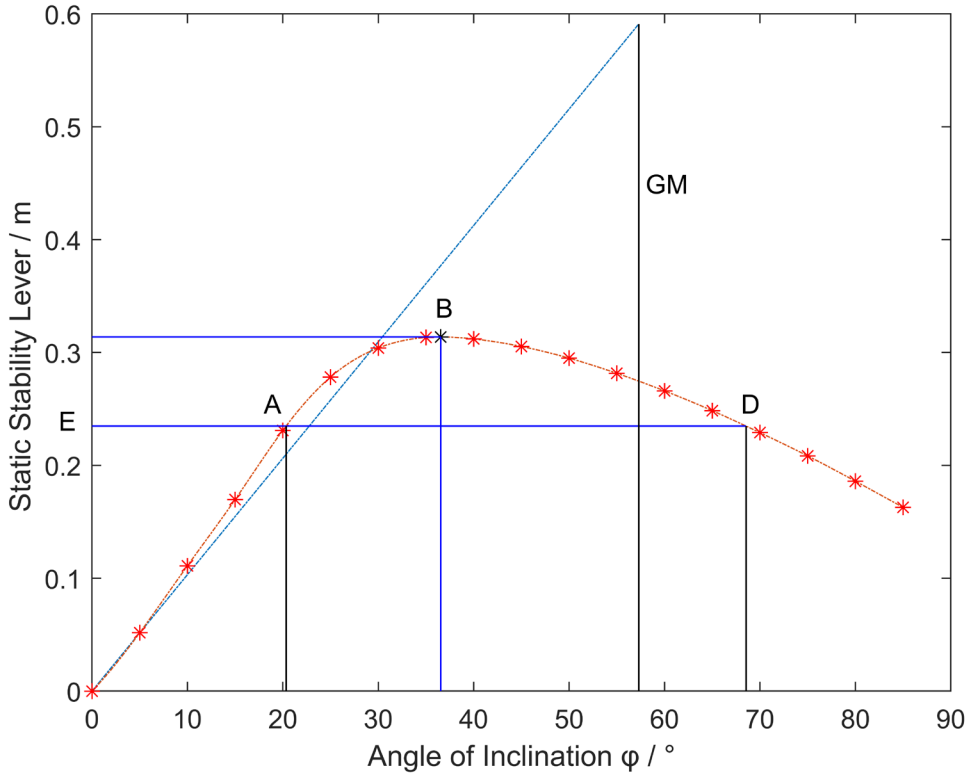

Figure 7. Static stability lever.

After calculation, the maximum static stability lever of the buoy is 0.3138 m, the corresponding limit static heeling angle is 36.55°, and the maximum restoring moment is 1599 N×m. The maximum free heeling angle of the buoy due to waves in the deployed sea area was calculated in Section 2.2.4. Obviously $\theta_{max} = 19° < \varphi_{max}$, if only under the action of waves, from the static stability curve, the stability of the buoy can still satisfy the influence of waves on it. However, the static stability curve only considers that the buoy is constantly and slowly acted upon by the external moment during the tilting process, and the angular acceleration is not considered. Apart from the constant current that will generate a constant moment on the buoy within a certain period, other external moments come from such things as the violent impact of waves, the ebb and flow of tides, and the sudden attack from the wind, which will change significantly in a short period, which will result in even these external moments being equal to the righting moment. The buoy would not stop tilting immediately but instead continue to tilt at a certain angle due to inertia. While the work performed by the external moment is equal to the work performed by the righting moment, the buoy will stop inclination, and the angle reached after stopping inclination is called the dynamic healing angle. Therefore, the angular acceleration and the dynamic stability performance must be considered when analyzing the buoy-restoring equilibrium process.

3.2. Dynamic Stability Curve

The dynamic stability of the buoy is expressed as the work performed by the righting moment of the buoy during the restoring equilibrium process [16]. When the buoy is tilted by φ_d, the calculation formula for the work performed by its restoring moment is written as follows:

$$T_R = V \times L_d = \int_0^{\varphi_d} M_R d\varphi = V \times \int_0^{\varphi_d} L d\varphi \tag{48}$$

$$L_d = \int_0^{\varphi_d} L d\varphi \tag{49}$$

where L_d is the dynamic stability lever and V is the displacement of the buoy.

The ordinate of the dynamic stability curve at $\varphi = \varphi_d$ is expressed as the area enclosed by the static stability curve and $\varphi = \varphi_d$. On the static stability curve in Figure 7, draw a horizontal line to make the area OAE equal to the area ABD, and point D is in the descending section of the static stability curve. At this time, the work performed by the external moment is equal to the work performed by the restoring moment. If the external torque increases again, the work performed by the two moments can no longer be offset, which will cause the buoy to overturn. Therefore this limit external moment is called the maximum wind heeling moment M_{OEMAX} or the minimum capsizing moment. The inclination angle corresponding to point D is called the limit dynamic heeling angle, while the inclination angle corresponding to point A is called the maximum dynamic stability rolling angle. After calculation, the limit dynamic heeling angle of the buoy designed in this paper is $\varphi_{dmax} = 68.55°$, the maximum dynamic stability heeling angle is $\varphi = 20.35°$, the corresponding maximum wind heeling arm is 0.2348 m, and the maximum wind heeling moment that can be supported is $M_{OEMAX} = 1196\ N \times m$ (Figure 8).

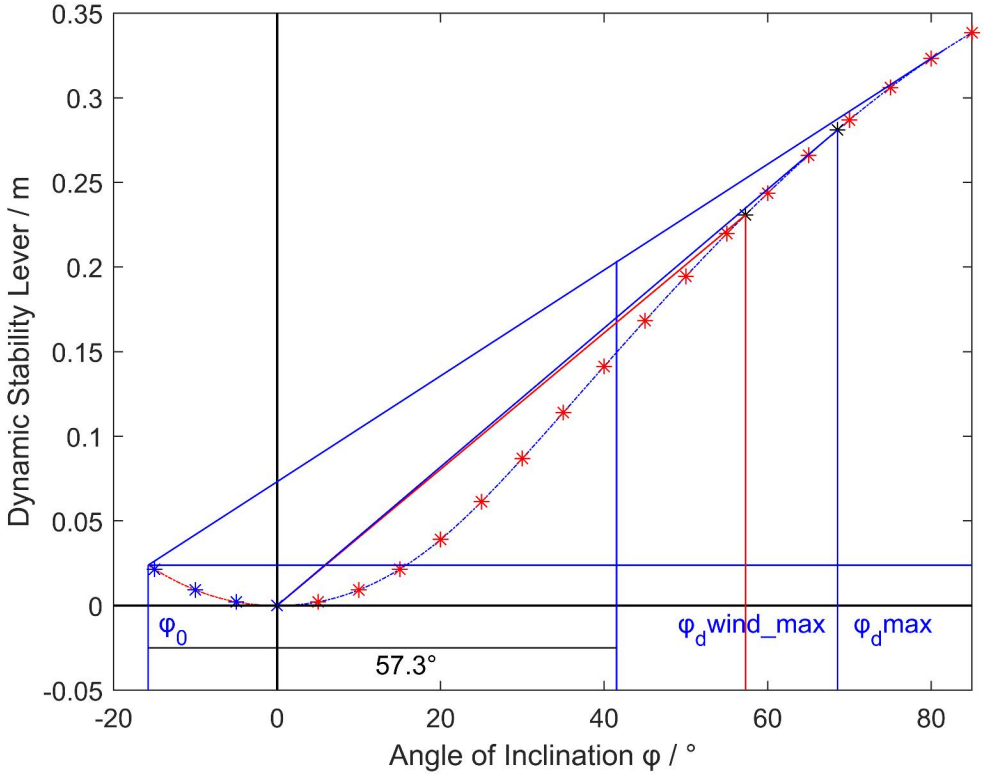

Figure 8. Dynamic stability lever.

According to the calculation formula for wind resistance, which is given by

$$F = \frac{1}{2} \times C \times \rho \times S \times v^2 \tag{50}$$

where C is the air resistance coefficient, taking the value of 1.6, ρ is the air density, taking 1.29 kg/m^3, S is the windward area of the buoy, v is the wind speed, and assuming that the windward area of the upper tower instrument is 0.3 m^2, the center of the windward area is 0.8 m from the waterline, the area above the waterline of the buoy is 0.56 m^2, and the distance to the waterline is 0.175 m, then wind speed v = 58 m/s might be derived by incorporating these values into the equation.

It can be seen that if only affected by the wind, the designed buoy could theoretically withstand a maximum wind speed of 58 m/s without overturning, which basically fulfills the industry standard for small buoys that can perform normally at wind speeds of less than 60 m/s.

However, the buoy cannot be only subjected to the wind or the wave; usually, it is frequently susceptible to both. Waves become more noticeable as the sea surface wind increases. Statistics show that the greatest wind speed in the sea area can reach level 8 severe winds of around 17–20 m/s. While the value of 20 m/s is brought into the above formula, the wind effect on the buoy is calculated to be 160 N×m, which causes the buoy to tilt to 6.18°. The restoring force arm is 0.065 m, and the restoring moment is 325 N×m. At this time, the combined effect of wind and waves should be divided into two situations to discuss.

Case 1: When the buoy is heeling to the maximum inclination angle of 6.18° caused by the wind, if the external moment exerted by a wave on the buoy is in the same direction as the righting moment after the action of the wind heeling moment, the inclination motion of the buoy will be aggravated under the action of two co-directional moments. Since the buoy is left-right symmetrical, the static and dynamic stability curves are symmetrical about the origin O. Taking OC1 = 6.18° in the static stability curve and making the horizontal line E1D1 to let $S_{C_1E_1A_1} = S_{A_1BD_1}$, the maximum tilting moment that the buoy can bear in this case, also known as the minimum overturning moment, is equal to 1090 N×m, and the limit dynamic healing inclination angle is 73.8°. If the external moment exerted by the wave on the buoy exceeds this limit value, the buoy may overturn.

Case 2: When the buoy is first shaken by the action of the wave and then inclined to the windward side to the maximum angle, in this moment, the buoy is about to roll back under the action of its restoring moment. If affected by the abovementioned wind heeling moment, the inclination of the buoy will also increase due to the same direction of both moments. In the second section, it has been determined that the maximum free rolling angle of the buoy in this sea area is 19°. Repeating the above calculation method to assume $S_{C_2E_2A_2} = S_{A_2BD_2}$ and then calculating the extreme dynamic heeling angle of the buoy at this time is 24.61° without danger of overturning (Figure 9).

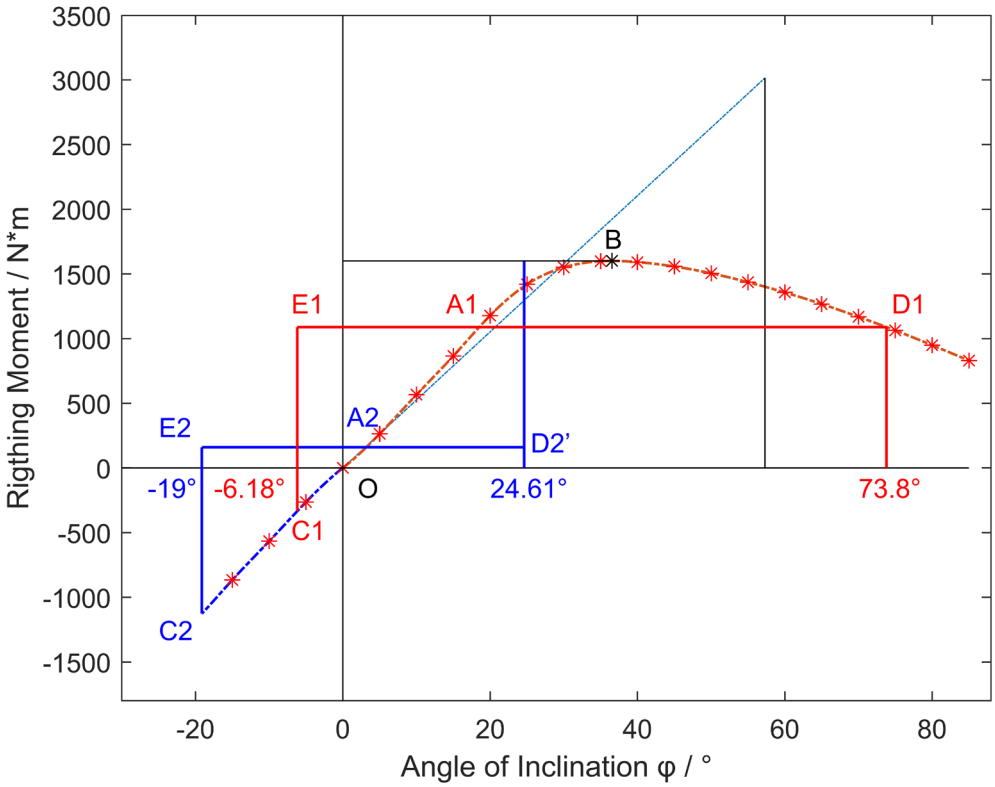

Figure 9. Righting moment of static stability.

3.3. Optimization of Buoy Structure

Increasing the weight and the draft of the buoy body would increase the restoring moment of the buoy [17]. To facilitate the placement of buoys at sea, the width of the buoys will not be changed. Under the same material used, increasing the height of the buoys to a certain extent can increase their weight and draft. However, it will also increase the center of gravity of the buoy, making the metacentric height and the static stability arm smaller, so a certain balance should be achieved between the two factors. Establish the buoys model with different ratios of width and height and then calculate their stability to obtain the following static stability moment curve, where the heights of the buoys are 40 cm, 60 cm, 80 cm, and 100 cm, respectively, with the same width of 1.6 m (Figure 10).

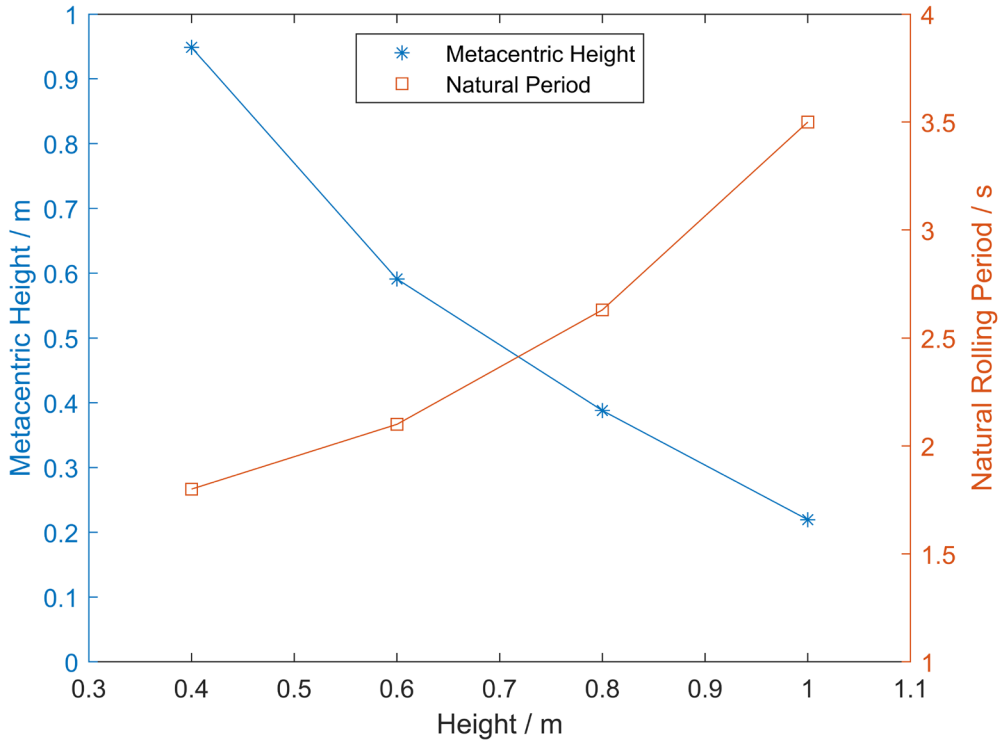

Figure 10. The relationship between metacentric height, natural period, and height of the main floating body of the buoy.

With the increase in height, the metacentric height of the buoy will become smaller, as shown in Figure 11. While the height is 40 cm, the metacentric height reaches more than 0.9 m. However, the excessively high metacentric height will reduce the natural rolling period of the buoy, which will increase the frequency of the buoy's rolling motion when the buoy encounters wind and waves [18]. In addition, the righting moment of this buoy is smaller than that of other buoys, and while encountering a large external moment, the dynamic stability heeling angle of this buoy will be larger than that of others due to its poor dynamic stability performance. On the other hand, because of the small area above the waterline, this 40 cm high buoy has better wind resistance. When the buoy has a height of 100 cm, the metacentric height is only 0.21 m. Although the restoring moment is larger at large inclination angles, the wind-receiving area on the waterline and the flow-receiving area below the waterline are enlarged due to the higher buoy height, resulting in the capacity of resistance to an external moment with a small inclination angle less than 20° being worse than the other three sizes of buoys (Figures 12–15).

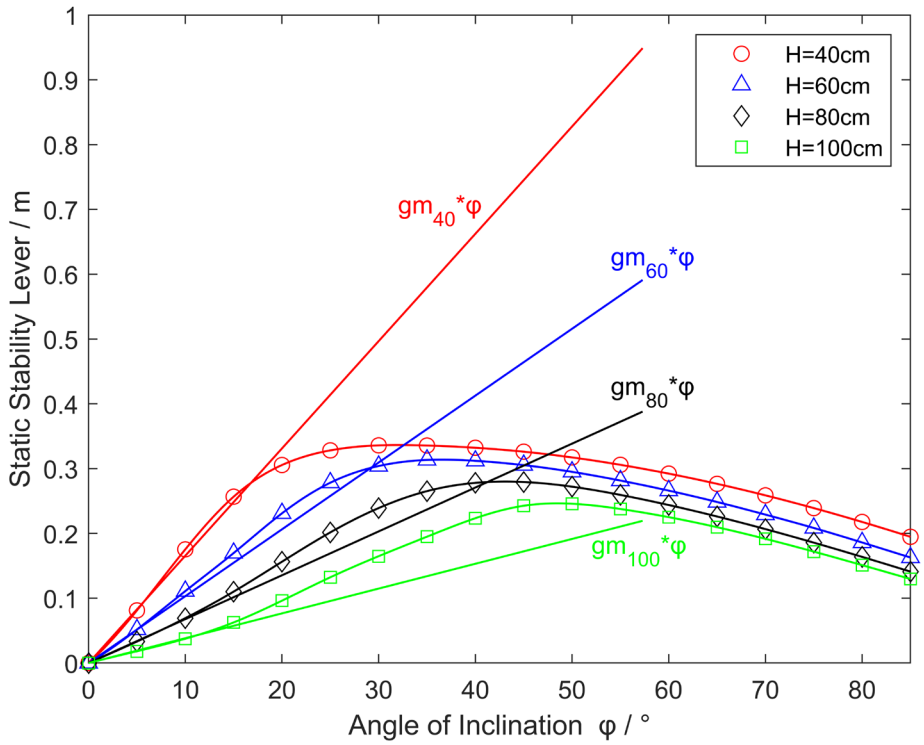

Figure 11. Static stability lever of the buoys with different heights.

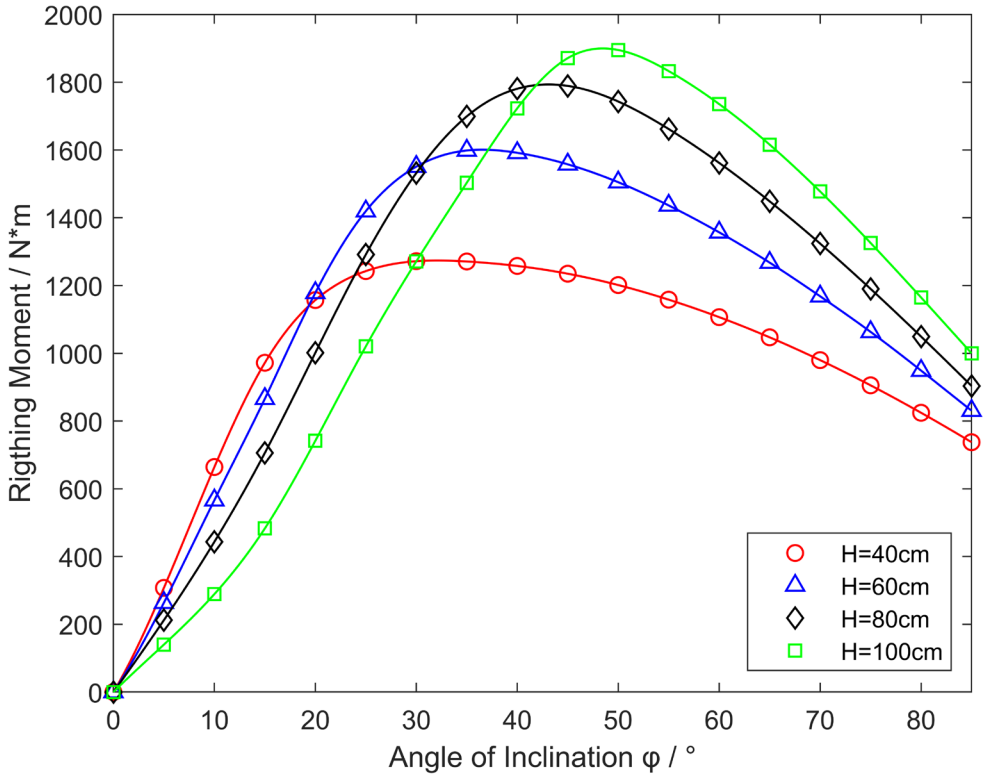

Figure 12. Righting moment of the buoys.

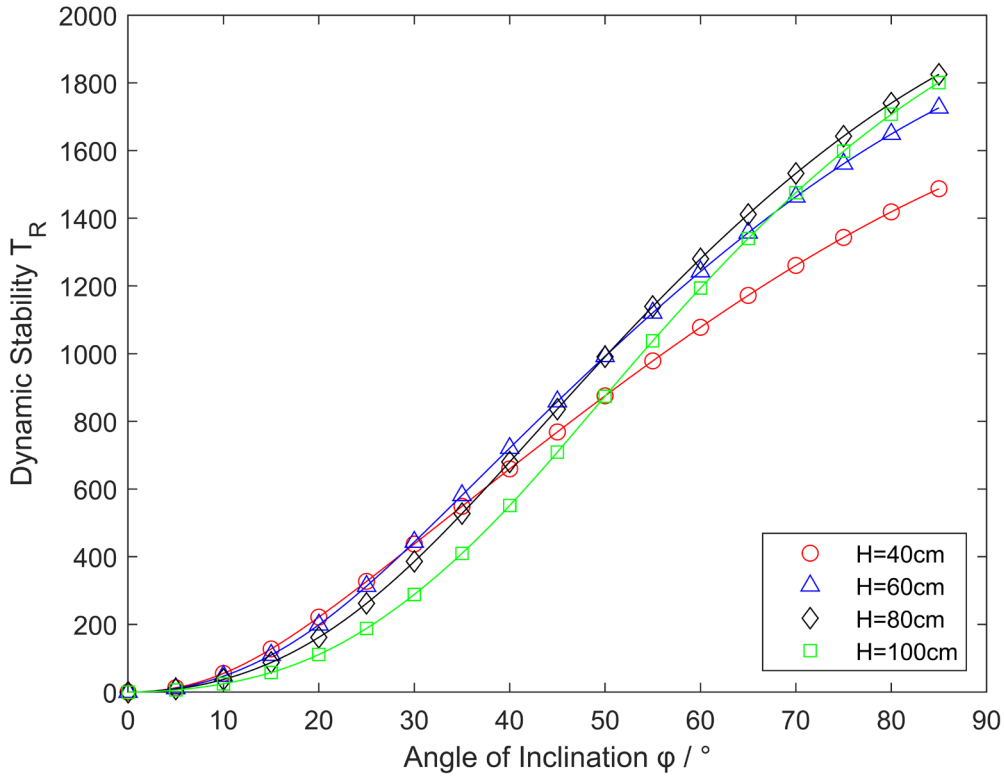

Figure 13. Dynamic stability of buoys.

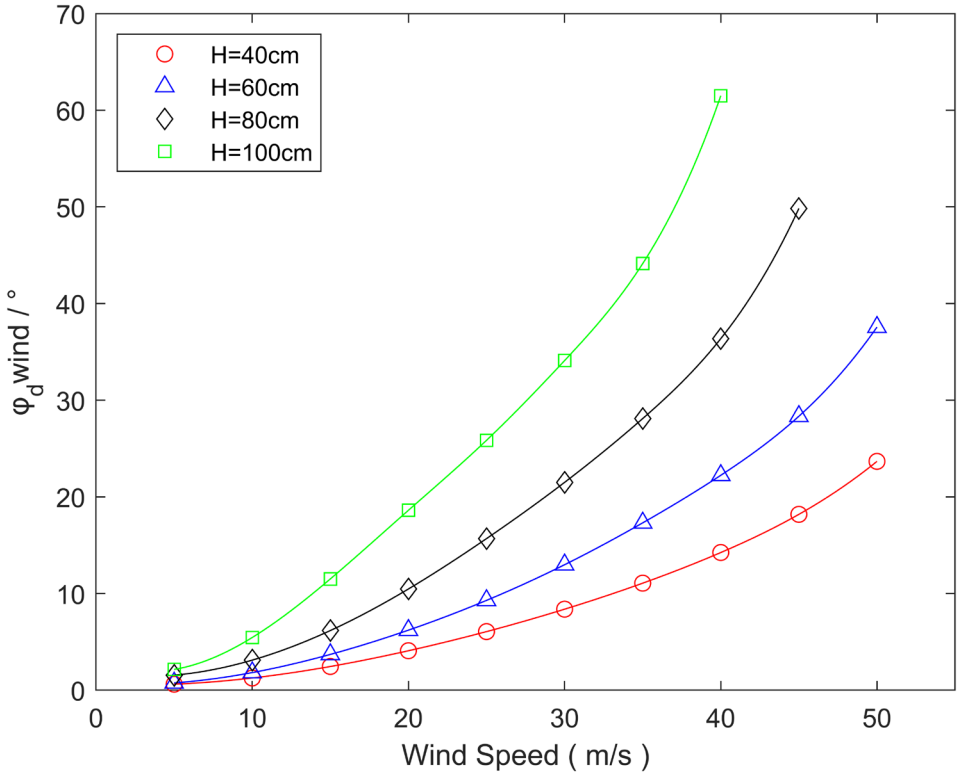

Figure 14. Dynamic heeling angle caused by wind.

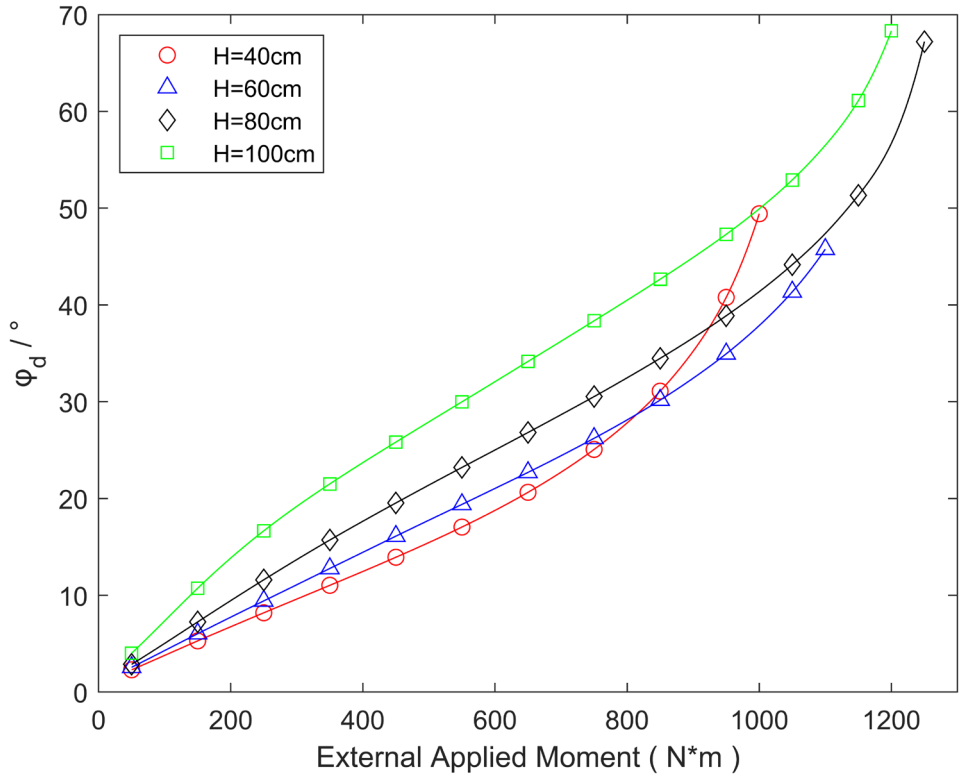

Figure 15. Dynamic heeling angle caused by the same external moment.

In Figure 16, the wave spectral function in the China Sea area is given by the following equation:

$$S_{xx}(\omega) = \frac{0.74}{\omega} \times \exp\left(-\frac{96.2}{u^2 * \omega^2}\right) \tag{51}$$

where ω is the angular frequency of the wave, and u is the sea surface wind speed.

The amplitude response density function of the buoy rolling motion is written as follows [19,20]:

$$S_{\theta\theta}(\omega) = RAO^2 \times S_{xx}(\omega) \tag{52}$$

$$RAO^2 = \frac{\omega^4}{g^2} \times \frac{1}{\left(1 - \left(\frac{\omega}{\omega_0}\right)^2\right)^2 + 4 \times \mu_0 \times \left(\frac{\omega}{\omega_0}\right)^2} \tag{53}$$

where RAO is the amplitude response operator, μ_0 is the damping coefficient, and ω_0 is the natural angular frequency of the rolling motion.

By calculating the spectral moments of the spectral function, several amplitudes and periods of the response motion of the buoy can be obtained, and the results are shown in Figures 17 and 18.

In Figures 19–22, the results of calculating methods and model simulation of the buoy are given by assuming a sea surface wind speed of 12 m/s in a class V sea state, where the first row shows the result of the rolling angle calculated by the simulation, the second row shows the time-domain and frequency-domain separation of the simulated data in 1 by FFT, the third row illustrates the rolling angle of the model simulation results given by the AQWA 14.0, and the fourth row displays the probability distribution of rolling angle.

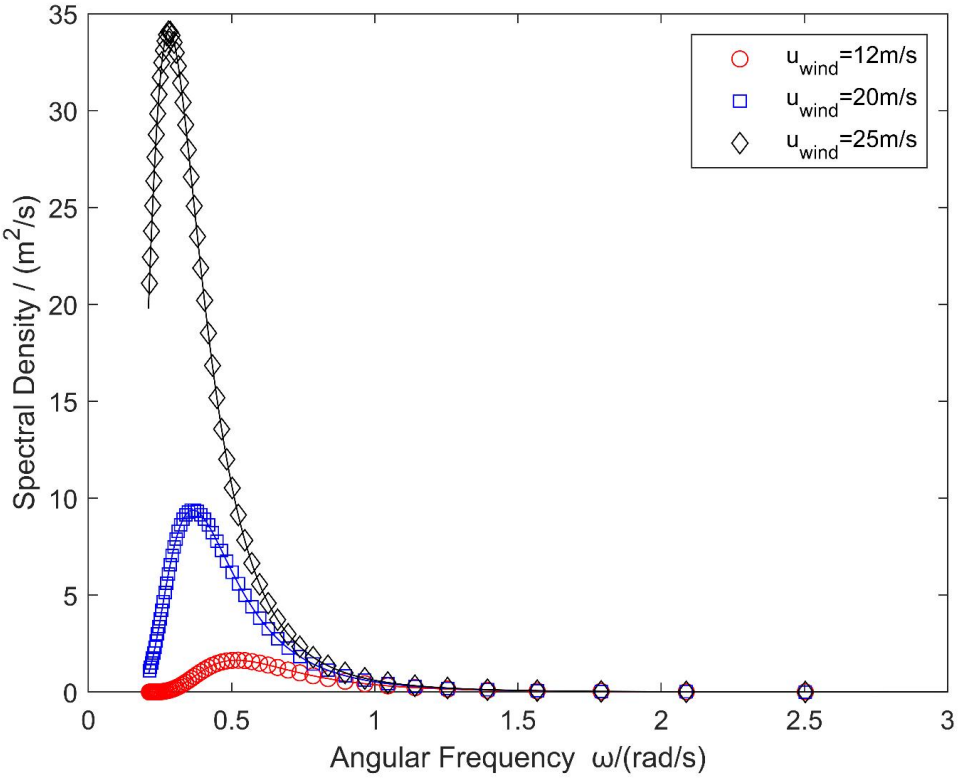

Figure 16. Wave spectrum in the China Sea area.

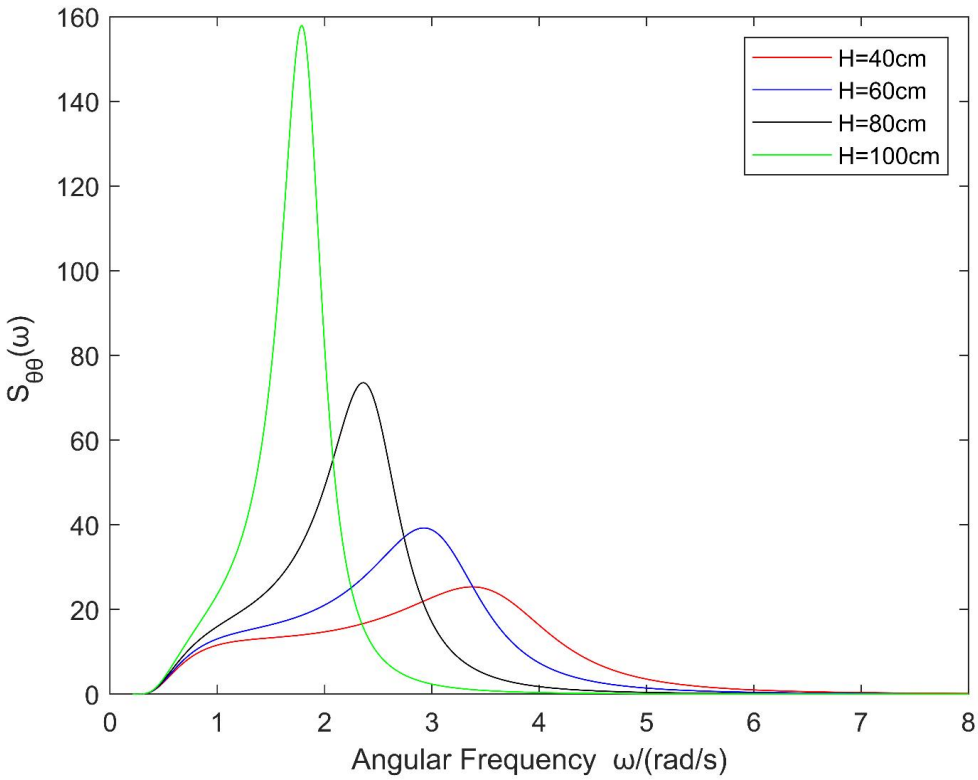

Figure 17. Frequency domain response spectrum of buoy rolling motion.

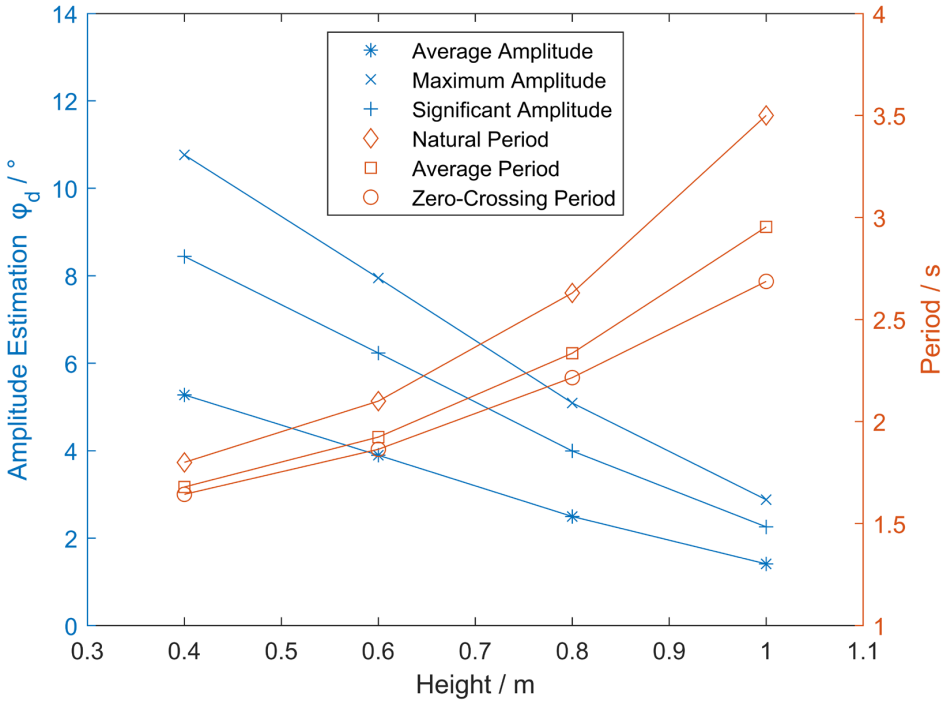

Figure 18. Statistics of rolling amplitude and period.

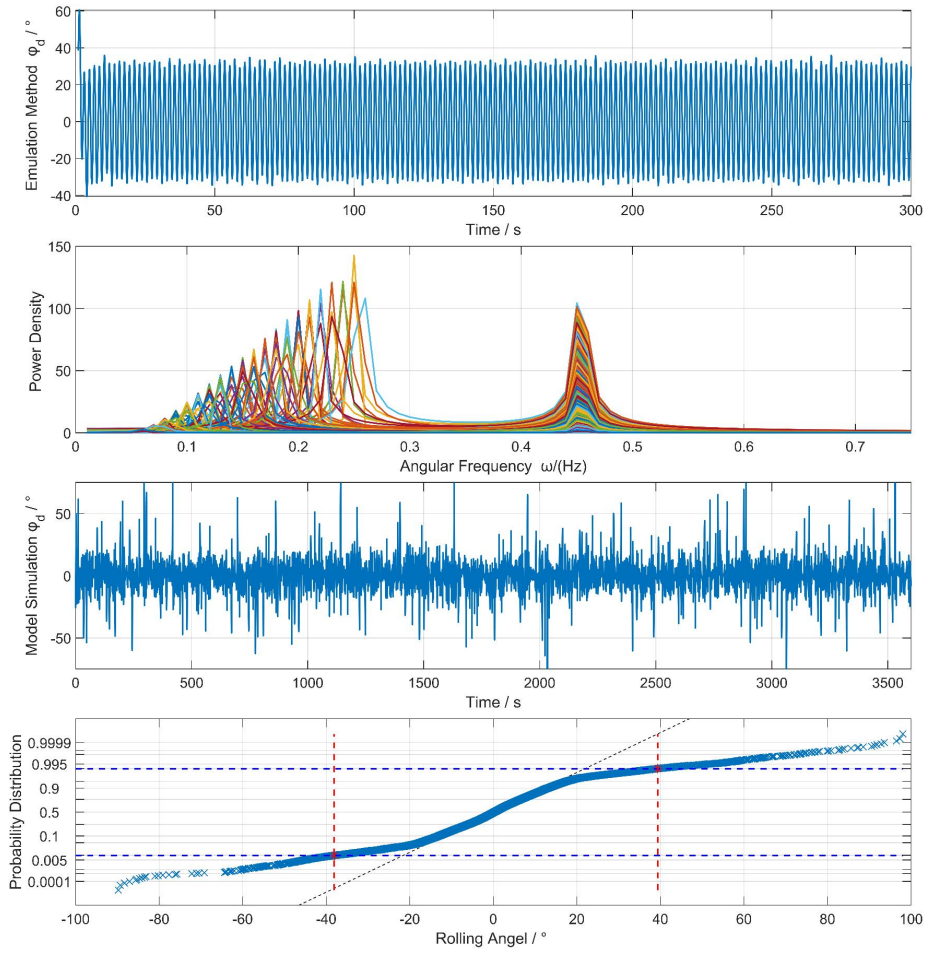

Figure 19. Frequency domain analysis of the rolling motion of a buoy with a height of 40 cm.

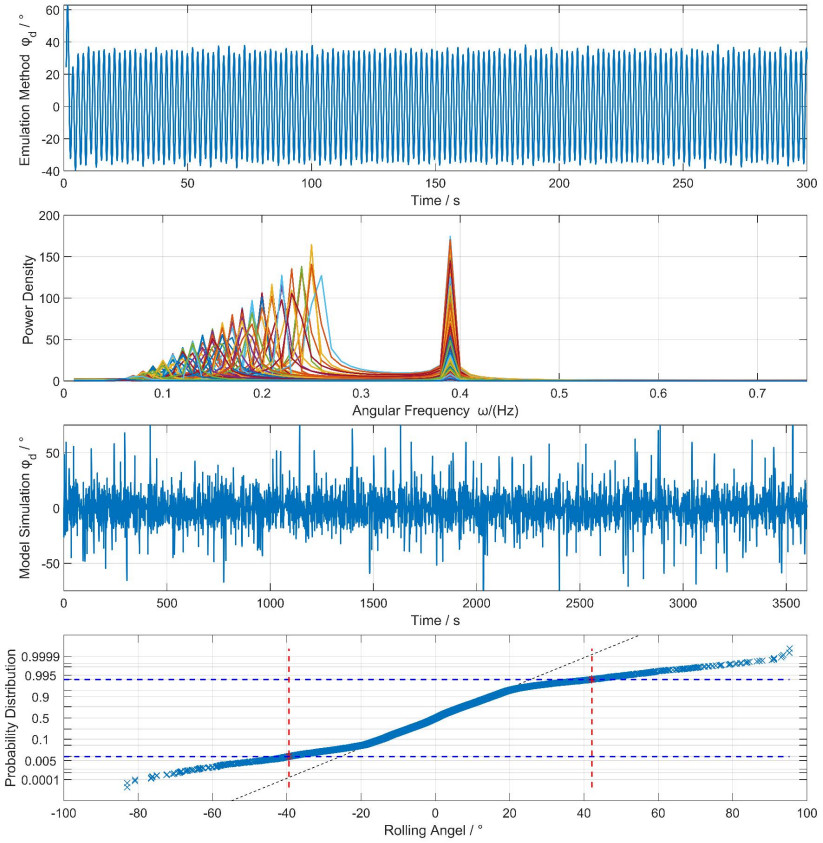

Figure 20. Frequency domain analysis of the rolling motion of a buoy with a height of 60 cm.

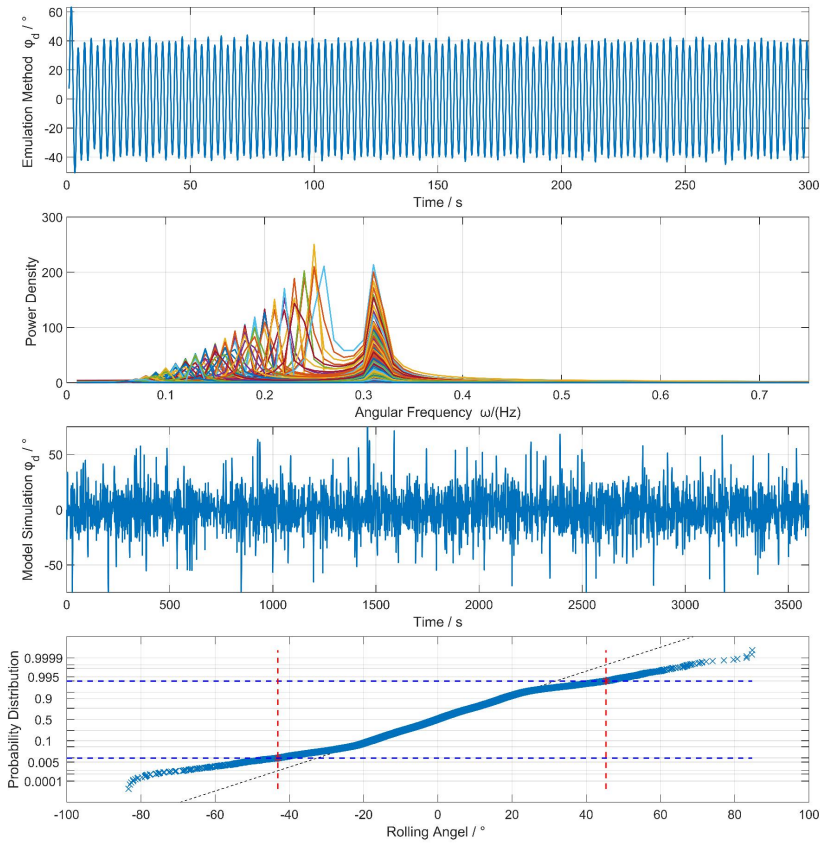

Figure 21. Frequency domain analysis of the rolling motion of a buoy with a height of 80 cm.

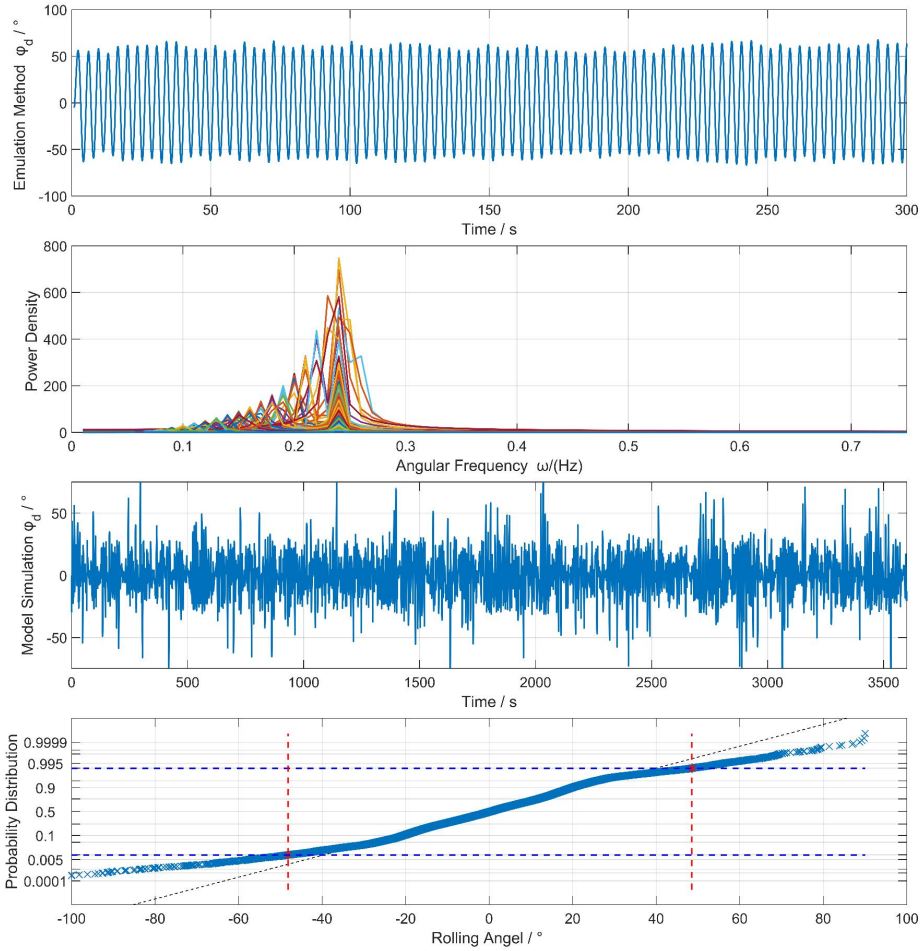

Figure 22. Frequency domain analysis of the rolling motion of a buoy with a height of 100 cm.

From the first row, it can be seen that with the increase in the height, the amplitude of the dynamic rolling angle of the buoy only in the ideal state of wave action gradually decreases and increases, indicating that its stability performance is negatively correlated with the height of the depth. And the separation of the frequency domain response by fast Fourier transform shows that when the natural angular frequency of the buoy is close to the wave frequency, the rolling response is obvious and severe, which illustrates that the response spectrum energy is substantially concentrated.

As observed from the time history distribution and probability distribution charts, it can be seen that under the conditions considering wind and irregular waves, the upper and lower limits of the rolling angle corresponding to the 98% statistical probability also increase with height. This indicates that with large buoy heights, the discrete fluctuations of the rolling response become more pronounced, leading to poorer dynamic stability.

Therefore, the buoy has relatively large righting moment and dynamic stability performance at the height range of 60–80 cm, as well as a good balance of wind resistance, resistance to external moment, and resistance to wave disturbance, indicating that the designed buoy in this paper is more reasonable in size and has sufficient stability performance. Finally, it can be concluded that without changing the type of material used for the main floating body, the buoy will perform better in terms of stability when the ratio of height to a definite width is between 0.375 and 0.5. Similarly, the same is the case at a certain height with a different width.

4. Conclusions

The inherent parameters of the designed buoy are obtained after the above numerical calculation. Taking the bottom of the main floating body as the reference plane, the center of gravity of the buoy is 13 cm high, the center of buoyancy is 9 cm high at stable equilibrium, and the height of the waterline surface is 25 cm. The natural rolling period of the buoy is 5.5 s. The maximum free heeling angle is 32° under the action of waves in the released sea area, and it can withstand the wind speed of 58 m/s without capsizing. The stability parameters are as follows: the metacentric height of the buoy is 0.591 m, the metacentric radius is 0.631 m, the limit static heeling angle is 36.55°, the maximum righting moment is 1599 N×m, and the maximum wind heeling moment that it can withstand is 1196 N×m. So this suggests that the buoy designed in this paper has excellent stability performance, and the restoring moment can fully cope with the tilting of the buoy caused by various winds and waves in the sea area without overturning. Finally, a parametric study of the buoy is further analyzed, which showed that without changing the material used for the main floating body, the buoy with a height-to-width ratio of 0.375–0.5 will have a relatively balanced stability performance.

This study aims to establish a complete and universally applicable integral model and ideas to analyze the stability of cylindrical buoys and also provide a reference for other types of buoys, which indicated that just changing the integral of the calculated model and using programming software to solve it could easily obtain the stability performance of research object buoys. However, the mooring system of the buoy and other disturbances of the ocean, such as currents and tidal currents, have not been considered in the analysis in this paper, whose effects are relatively small relative to wind and waves. However, these influencing factors would be further refined and incorporated into the analysis in future studies on hydrodynamic analysis.

Author Contributions: Conceptualization, Y.C. and Y.L.; Methodology, H.Z. and Y.L.; Software, H.Z. and Q.L.; Validation, Q.L.; Formal analysis, Z.Z. and M.L.; Investigation, H.Z., Y.C., Q.L. and Y.L.; Writing—original draft, H.Z. and Z.Z.; Writing—review & editing, M.L.; Visualization, H.Z.; Supervision, Y.C. and Y.L.; Project administration, Y.C. and Y.L.; Funding acquisition, Y.C. and Y.L. All authors have read and agreed to the published version of the manuscript.

Funding: This study was supported by the National Key R&D Program of China (No. 2022YFC3104102), the National Key R&D Program of China (No. 2022YFC3104200), the Key R&D Program of Shandong Province, China (No. 2023ZLYS01), and the Innovation Project of Qingdao Post-Doctoral (QDBSH20230202121).

Institutional Review Board Statement: Not applicable.

Informed Consent Statement: Not applicable.

Data Availability Statement: Data are contained within the article.

Conflicts of Interest: The authors declare no conflict of interest.

References

1. Mills, D.K.; Laane, R.W.; Rees, J.M.; van der Loeff, M.R.; Suylen, J.M.; Pearce, D.J.; Sivyer, D.B.; Heins, C.; Platt, K.; Rawlinson, M. *Smartbuoy: A Marine Environmental Monitoring Buoy with a Difference*; Elsevier Oceanography Series; Elsevier: Amsterdam, The Netherlands, 2003; Volume 69, pp. 311–316.
2. Zhang, H.; Zhang, D.; Zhang, A. An Innovative Multifunctional Buoy Design for Monitoring Continuous Environmental Dy-namics at Tianjin Port. *IEEE Access* **2020**, *8*, 171820–171833. [CrossRef]
3. Pillai, A.C.; Davey, T.; Draycott, S. A framework for processing wave buoy measurements in the presence of current. *Appl. Ocean Res.* **2021**, *106*, 102420. [CrossRef]
4. Wang, J.C.; Li, Y.Z. Development and application of ocean data buoy technology in China. *Shandong Sci.* **2019**, *32*, 1–20.
5. Sun, C.; Chen, Z.; Ning, C.; Mou, S. Research on Key Problems of Ocean Data Buoy. *J. Hangzhou Dianzi Univ.* **2013**, *33*, 146–149.
6. Molland, A.F. Chapter 3—Flotation and stability. In *The Maritime Engineering Reference Book*; Butterworth-Heinemann: Oxford, UK, 2008; pp. 75–115.
7. Li, X.; Jin, H.; Zhao, X.; Chen, J.; Tong, J.; Fen, Z.; Li, H. Hydrodynamic Characteristics Analysis of Sea Buoy Pitch Motion in Waves. In Proceedings of the 2018 OCEANS—MTS/IEEE Kobe Techno-Oceans (OTO), Kobe, Japan, 28–31 May 2018.

8. Wang, J.; Wang, Z.; Wang, Y.; Liu, S.; Li, Y. Current situation and trend of marine data buoy and monitoring network technology of China. *Acta Oceanol. Sin.* **2016**, *35*, 1–10. [CrossRef]
9. Liang, G.; Xue, Y.; Sun, B.; Tao, C.; Guan, S.; Zhou, X. Stability Design of Small Buoy for Marine Physical Property Monitoring. *Adv. Mar. Sci.* **2020**, *38*, 541–548.
10. Li, C.; Li, Y.; Yi, H. Study on the initial stability of canted strut SWATH. *Ship Eng.* **2009**, *31*, 6–8.
11. Li, X.-j.; Xie, X.-l.; Zhao, J. The influencing factors of semi-submersible vessel's metacentric height limits and mechanism of action. *J. Harbin Eng. Univ.* **2015**, *36*, 109–112.
12. Li, H.; Xu, C.; Tian, Y.; Qu, F.; Chen, J.; Sun, K.; Leng, J.; Wei, Y. The design of a novel small waterplane area pillar buoy based on rolling analysis. *Ocean Eng.* **2019**, *184*, 289–298. [CrossRef]
13. Berteaux, H.O. Buoy engineering. In *Ocean Engineering*; Wiley Series; Wiley: New York, NY, USA, 1976.
14. Wang, J.C. *Principle and Engineering of Ocean Data Buoy*; China Ocean Press: Beijing, China, 2013; pp. 39–45.
15. Radhakrishnan, S.; Datla, R.; Hires, R.I. Theoretical and experimental analysis of tethered buoy instability in gravity waves. *Ocean Eng.* **2007**, *34*, 261–274. [CrossRef]
16. Sheng, Z. *Ship Principle*; Shanghai Jiao Tong University Press: Shanghai, China, 2017; Volume 2, pp. 23–122.
17. Qu, S.-C.; Zheng, K.; Wang, Y.-M. Analysis and Simulation of Spar Buoy Motion. *Comput. Simul.* **2010**, *27*, 363–367.
18. Xu, C.; OBI, O.J.; Li, H.; Tian, Y.; Zheng, S.; Leng, J.; Shuo, L. Structural design and analysis of small waterplane area buoy. In Proceedings of the OCEANS 2019—Marseille, Marseille, France, 17–20 June 2019.
19. Ibinabo, I.; Tamunodukobipi, D.T. Determination of the Response Amplitude Operator (s) of an FPSO. *Engineering* **2019**, *11*, 541–556. [CrossRef]
20. Ramachandran, G.K.V.; Robertson, A.; Jonkman, J.M.; Masciola, M.D. Investigation of Response Amplitude Operators for Floating Offshore Wind Turbines. In Proceedings of the Twenty-Third International Offshore and Polar Engineering Conference, Anchorage, Alaska, 30 June–5 July 2013.